[Article ID] 1003- 6326(2002)04- 0686- 05

High temperature creep behavior of in-situ synthesized $MoSi_2$-30%SiC composite①

FU Xiao-wei(傅晓伟)[1], YANG Wang-yue(杨王玥)[1], SUN Zu-qing(孙祖庆)[2],
ZHANG Lai-qi(张来启)[2], ZHU Jing(朱 静)[3]
(1. School of Materials Science & Engineering,
University of Science & Technology Beijing, Beijing 100083, China;
2. State Key Laboratory for Advanced Metals and Materials,
University of Science & Technology Beijing, Beijing 100083, China;
3. Department of Materials Science & Engineering, Tsinghua University, Beijing 100084, China)

[Abstract] The compressive creep behavior at 1200~ 1400 ℃ of an in-situ synthesized $MoSi_2$-30% SiC (volume fraction) composite and a traditional PM $MoSi_2$-30% SiC (volume fraction) composite is investigated. The creep rate of the in-situ synthesized $MoSi_2$-30% SiC (volume fraction) composite is about $10^{-7}s^{-1}$ under stress of 60~ 120 MPa, and significantly lower than that made by PM method above 1300 ℃. The reason is that the interface between SiC particle and $MoSi_2$ matrix in in-situ synthesized $SiC_p/MoSi_2$ is of direct atomic bonding without any amorphous glassy phase, such as SiO_2 structure. Creep deformation occurs primarily by dislocation motion and the dislocations have Burgers vectors of the type of ⟨110⟩ and ⟨100⟩.

[Key words] SiC/$MoSi_2$ composite; in-situ synthesis; creep; dislocation
[CLC number] TG 113.25; TG 148 [Document code] A

1 INTRODUCTION

The reaction thermodynamics sequence of the phase formation and the microstructure in the in-situ reactive sintering in Mo-Si-C ternary system were systematically investigated. Based on these fundamental studies, $MoSi_2$ based composites reinforced by SiC particle have been successfully synthesized. The interface in the composites has been confirmed to be clean[1~4]. The investigation on mechanical behavior of in-situ synthesized $SiC_p/MoSi_2$ composite have shown that the fracture toughness, Vickers hardness at room temperature and high temperature compressive strength are significantly higher than those of monolithic $MoSi_2$ and commercial powder metallurgical $SiC_p/MoSi_2$ composites[5~7]. To date, there have been relatively few studies on the relation between creep properties and microstructure of $MoSi_2$ composites. This paper concentrates on creep behavior and mechanism of in-situ synthesized $SiC_p/MoSi_2$ composite at 1200~ 1400 ℃.

2 EXPERIMENTAL

Two materials are included in this study: a composite reinforced with 30% SiC (volume fraction) synthesized in-situ and a powder metallurgy (PM) $MoSi_2$-30% SiC (volume fraction) composite fabricated by consolidating a commercial $MoSi_2$ powder and SiC powder. Both materials were produced by hot-pressing the composite powder at 1740 ℃ and 40 MPa for 2 h in Ar. $1HNO_3$+ 4HF+ $2H_2O$ reagent was used to etch the grain boundaries of $MoSi_2$ grains in the composite. Microstructures are examined by optical microscope, S-250, H-800 and JEOL-2010F. The size and spacing of the SiC particles are measured using IAS-4 image analysis system.

Archimedes method was used to calculate the bulk density of these materials with a precision of 0.0001 g. The porosity of the samples is given by

$$\theta = (1 - \rho/\rho_0) \times 100\% \quad (1)$$

where ρ is the actual density and ρ_0 is the theoretical density of the materials. The theoretical density of the composite can be given by

$$\rho = \sum \rho_i V_i \quad (2)$$

where ρ_i and V_i are theoretical density and volume fraction of the phase i. The theoretical density of $MoSi_2$ and SiC are 6.27 g/cm^3 and 3.27 g/cm^3, respectively.

The compression creep specimens were rectangular parallelepiped with dimension of 3.0 mm × 3.0 mm × 6.0 mm cut from the original disks. Compressive creep experiments were conduted at 1200~ 1400 ℃ in vacuum under applied stress of 60 ~ 120 MPa. Upon completion of a test, specimens were cooled rapidly under stress to retain the deformation

① [Foundation item] Project (59895150- 04- 02) supported by the National Natural Science Foundation of China
[Received date] 2001- 10- 08

microstructure. Thin foil TEM specimens were prepared by sectioning a disk from the center of each rectangular parallele-piped specimen and were examined using a Hitachi H-800 operated at 120 kV. High resolution electron microscopy (HREM) experiments are carried out using a JEOL-2010 operated at 200 kV.

3 RESULTS AND DISCUSSION

3.1 Microstructure

In the TEM image of the in-situ synthesized $SiC_p/MoSi_2$ composite, it can be seen that white SiC particles mainly distribute on grain boundaries of the $MoSi_2$ matrix and especially triple-point junctions. The SiC particles, sized 2 ~ 5 μm, are generally spherical or equiaxed, with some facet characteristics (as shown in Fig. 1(a))[8,9]. As it is observed in the lattice image of the in-situ synthesized $MoSi_2$-30% SiC composite, the bonding between $MoSi_2$ and SiC is directly atomic, without any amorphous structure of the SiO_2 type (as shown in Fig. 2). The bonding energy at the $MoSi_2$/SiC interface is higher than that at the $MoSi_2/SiO_2$ interface, hence the resistance against crack propagation is enhanced. The interface is characterized as an atomically flat semi-coherent interface, indicated by double arrows in Fig. 2, which consists of the coherent areas and misfit dislocations among these areas in the SiC phase side. As a result, the applied load can be effectively transferred to the SiC without decohesion and the interface energy is lower. However, there is a 0.5 ~ 1.5 nm amorphous layer at the interface in the composite that is prepared by the PM method or XDTM technique[10]. The binding between the matrix and the strengthening phase decreases due to the existence of an amorphous layer at the interface.

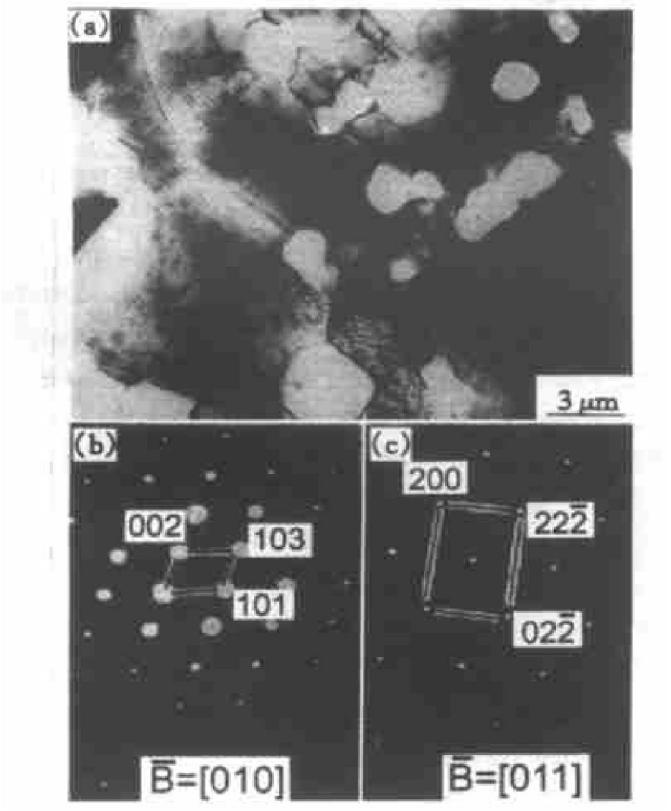

Fig. 1 TEM morphology of in-situ synthesized $MoSi_2$-30% SiC composite (a), EDPS of black matrix $MoSi_2$(b) and white particles SiC (c)

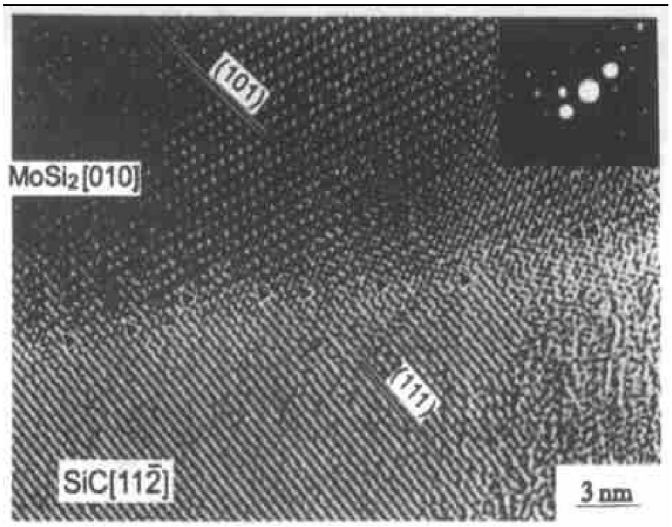

Fig. 2 HREM image of in-situ synthesized $MoSi_2$-30% SiC composite
(Double arrows show boundary between $MoSi_2$ and SiC, and single arrows are locations of misfit dislocation)

The size, spacing of SiC particles and porosities of two materials are described in Table 1. The results show that the porosity of the PM material is higher than that of the in-situ synthesized material. In the PM materials the SiC particles are nonuniformly distributed. Some black particles (indicated by the arrows in Fig. 3) have been found in the $MoSi_2$ matrix, which are confirmed to be SiO_2 by EDS and EDPS. These SiO_2 particles lead to high porosity in PM materials, about (0.864 ±0.179) %, which is originated from SiO_2 films on the starting $MoSi_2$ and SiC powder surfaces during the fabrication. However, the porosity of the in-situ synthesized material is only (0.044 ±0.014) %.

Table 1 Microstructure characteristics of in-situ synthesized and conventional PM $MoSi_2$-30% SiC composite

Processed method	Porosity / %	Mean size of SiC particles/ μm	Mean spacing of SiC particles/ μm
In-situ synthesized	0.044 ±0.014	2.70 ±1.45	5.72 ±4.07
Powder metallurgy	0.864 ±0.179	2.35 ±1.34	4.79 ±4.07

3.2 High temperature creep behavior

Fig. 4 and Fig. 5 show the compressive stress — strain curves for above two composites at 1400 ℃ and 1300 ℃ respectively. High temperature compressive steady-state creep rates are given in Table 2. The

Table 2 High temperature compress steady-state creep rates of in situ synthesized and conventional PM $MoSi_2$-30% SiC composite

$SiC_p/MoSi_2$ composite	Steady-state creep rate/s^{-1}					
	1 400 ℃	1 300 ℃			1 250 ℃	1 200 ℃
	80 MPa	80 MPa	100 MPa	120 MPa	120 MPa	120 MPa
In-situ synthesized	9.7×10^{-7}	2.2×10^{-7}	4.2×10^{-7}	8.3×10^{-7}	3.7×10^{-7}	1.5×10^{-7}
PM	3.6×10^{-6}	2.5×10^{-7}	5.4×10^{-7}			

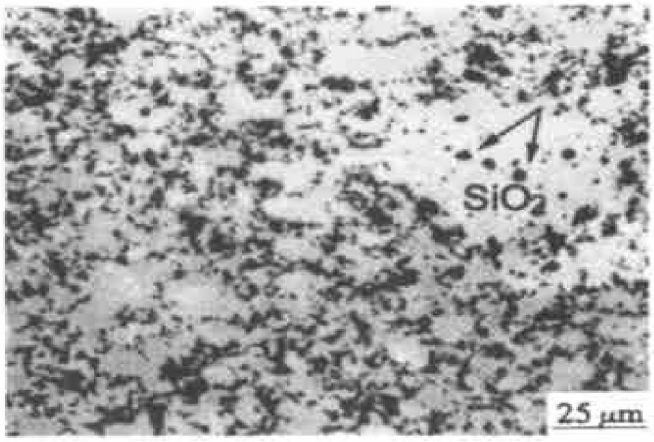

Fig. 3 Optical micrograph of PM $MoSi_2$-30% SiC composite

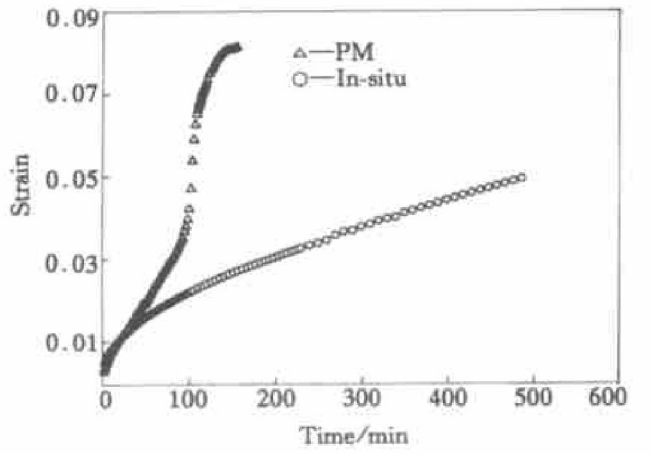

Fig. 4 Creep curves for in-situ synthesized and PM $MoSi_2$-30% SiC composite under stress of 80 MPa at 1 400 ℃

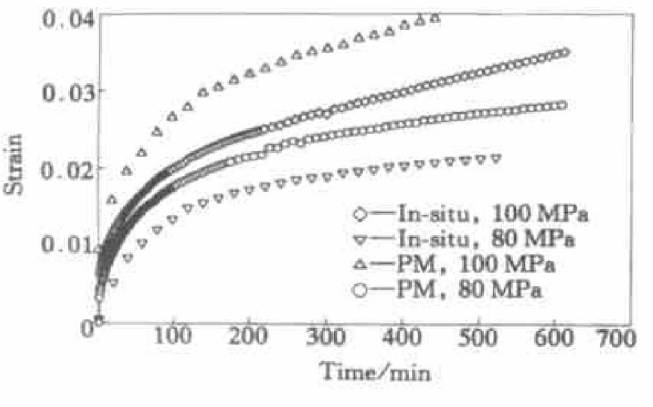

Fig. 5 Creep curves for in-situ synthesized and PM $MoSi_2$-30% SiC composite at 1 300 ℃

results show that in-situ synthesized $SiC_p/MoSi_2$ composites are more applicable at high temperatures especially above 1 400 ℃ due to high creep resistance. At 1 200~ 1 400 ℃ and 60~ 120 MPa, the steady creep rates of the in-situ synthesized materials is $10^{-7}s^{-1}$. The result at 1 300 ℃ and 80 MPa reveals that the high temperature creep resistance of the in-situ synthesized material is similar to that of the XD™ composite material[10] and is higher than that of hot-pressed whisker reinforced composite made at Los Alamos National Laboratory[11], despite the difference in volume fraction (20% whiskers vs. 30% particles). However, the steady creep rate of the conventionally PM materials in the same conditions is obviously higher than that of in-situ synthesized materials due to the high porosity which results in the diffusion of the vacancy and movement of atoms. At 1 400 ℃ and 80 MPa, the steady creep rate of the PM materials increases to $5.4\times10^{-6}s^{-1}$ (as shown in Fig. 4). It is believed that the creep behavior of the PM composites changed above 1 300 ℃ due to the impurity concentration and the softening of amorphous phase films along $MoSi_2$ grain boundaries formed during the fabrication, which causes interface to slide easily.

The steady creep rates are achieved for a range of stress levels from 60 MPa to 120 MPa at 1 300 ℃, and these are plotted as a function of applied stress in Fig. 6. Other creep data of a 20% SiC whisker-reinforced $MoSi_2$ and XD™ 30% $SiC_p/MoSi_2$ composite under the same condition are also given as a comparison. The creep data indicate power-law type constitutive behavior, i.e. $\sigma^n \propto \dot{\varepsilon}$. The stress exponent of the in-situ synthesized material is approximately 3.0, and that of the conventionally PM material is 4.0. In other work, Sadanada et al[11] reported that the exponent n value was about 3 for the 20% SiC whisker-reinforced $MoSi_2$ at 1 200~ 1 400 ℃, Suzuki et al reported 3.5 for the 30% SiC XD™ composite at 1 050 ~ 1 300 ℃ and Lavernia et al reported 2.5 for the low pressure plasma sprayed 9% SiC/$MoSi_2$ (volume fraction) below 1 300 ℃ and 1.5 above 1 300 ℃[12].

Apparent creep activation energies are calculated from creep rate and temperature under selected pressure according to the Arrheniu function:

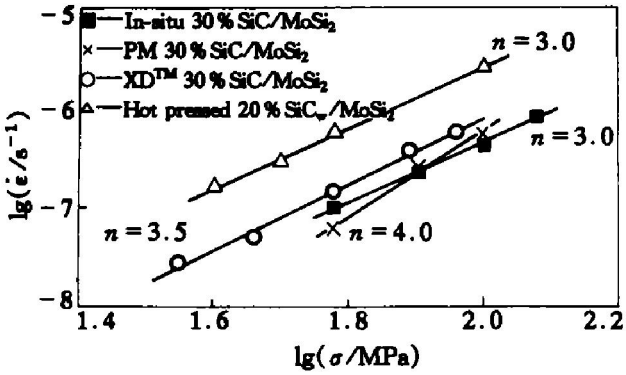

Fig. 6 Comparison of creep data obtained presently and reported in Refs. [10] and [11] at 1 300 ℃

$$\Delta G = R \ln \frac{\dot{\varepsilon}_1}{\dot{\varepsilon}_2} / \left(\frac{1}{T_2} - \frac{1}{T_1}\right) \quad (3)$$

The apparent creep activation energies for the in-situ synthesized $SiC_p/MoSi_2$ composite is 330 kJ/mol (as shown in Fig. 7). Lavernia et al[12] reported 300 kJ/mol for the low pressure plasma sprayed $MoSi_2$-9% SiC (volume fraction) below 1 300 ℃ and 190 kJ/mol above 1 300 ℃[12]. Other researchers reported 300~ 600 kJ/mol[10, 11].

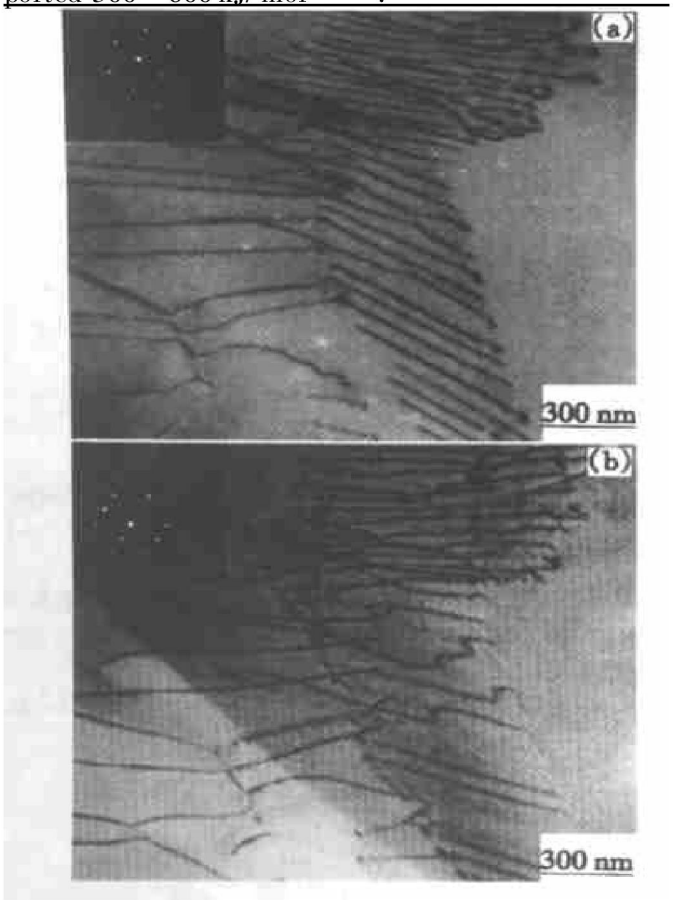

Fig. 7 Dislocation structure in in-situ synthesized $MoSi_2$-30% SiC composite after creep at 1 300 ℃ and 120 MPa
(a) —[331] zone axis; (b) —[110] zone axis

3.3 Creep mechanism

Generally, the creep mechanism can be determined by the values of stress exponent and apparent creep activation energy. That the exponent n is about 3 for the in-situ synthesized materials and 4 for the commercially PM materials indicates that the creep process is controlled by the dislocations motion.

The TEM investigation reveals that the density of matrix dislocations increases rapidly in the in-situ synthesized $SiC_p/MoSi_2$ composite samples after creep at 1 200~ 1 400 ℃. It is can be found also that these dislocations distribute nonuniformly and have a tendency to form the subgrain boundaries and networks. Dislocation substructures in the $SiC_p/MoSi_2$ composite after creep at 1 300 ℃ and 120 MPa are shown in Fig. 7(a) and (b) with zone axis of [331] and [110] respectively. Analysis of the dislocations reveals that the glide dislocations have Burgers vectors of the type ⟨100⟩ and ⟨110⟩, which is different from the results in the report for XDTM materials[10]. It can be concluded that ⟨100⟩ type dislocations glide during the creep process and ⟨110⟩ type dislocations climb and absorb the gliding dislocations which results in the formation of the subgrain boundaries and dislocation networks respectively. With the creep temperature increasing, the recovery and dislocation structures seem to occur apparently. The TEM image of the dislocation structures under different double-beam condition is shown in Fig. 8. Table 3 indicates the dislocation contrast regularity under different $\boldsymbol{g}$.

The interaction between $MoSi_2$ matrix and SiC particles can be found in the composites. The matrix dislocations pile up around the SiC particles, as

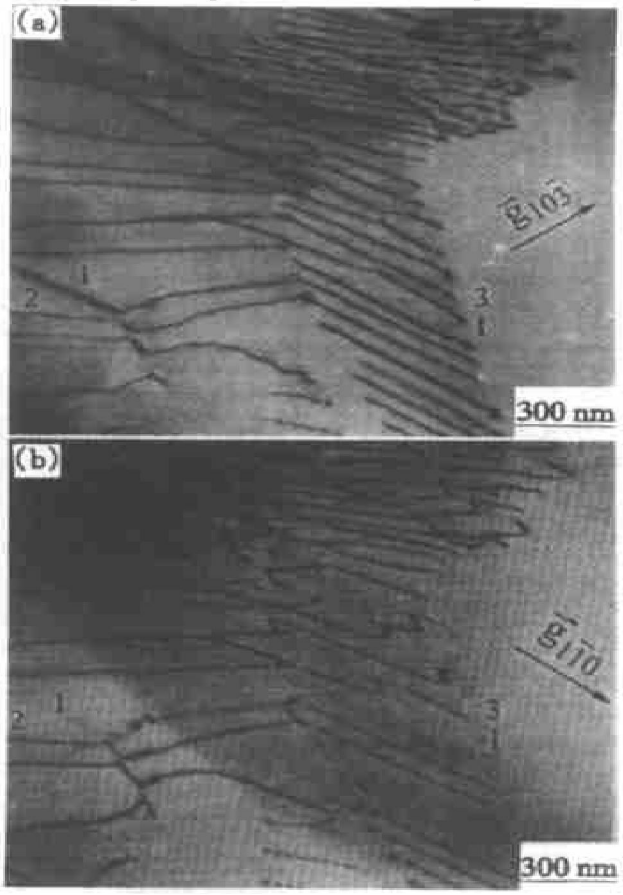

Fig. 8 TEM morphologies of dislocations
(a) —$\bar{g}$= [10$\bar{3}$]; (b) —$\bar{g}$= [1$\bar{1}$0]

Table 3 Dislocation contrast regularity taken with different g

Dislocation	g						Burgers vector
	$[2\bar{1}\bar{3}]$	$[0\bar{1}3]$	$[10\bar{3}]$	$1\bar{1}0$	$[1\bar{1}\bar{2}]$	$[\bar{1}10]$	
Type 1	Visible	Visible	Visible	Invisible	Invisible	Invisible	[110]
Type 2	Visible	Invisible	Visible	Visible	Visible	Visible	[100]
Type 3	Visible	Invisible	Visible	Visible	Visible	Visible	[100]

shown in Fig. 9. Glide during creep is impeded by the SiC particles around the grain boundaries, which produces dislocation tangles and pileups and then affects the dislocations motion in the adjacent $MoSi_2$ matrix. The reason why the steady creep rates in PM composites and XD^{TM} composites are higher is that the existence of the SiO_2 films promotes the interfaces glide and attenuates the pinning resulted from the SiC particles, which in turn reduces the high temperature creep resistance.

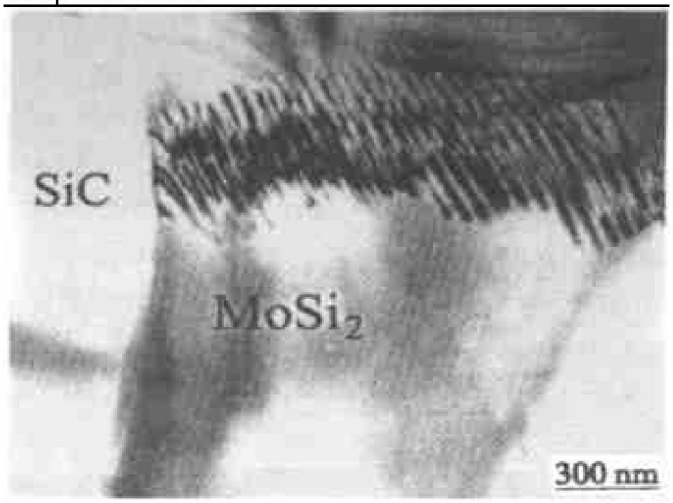

Fig. 9 Dislocation wall in front of particle SiC in in-situ synthesized $MoSi_2$-30% SiC composite after creep at 1 300 ℃ and 120 MPa

[REFERENCES]

[1] SUN Zu-qing, ZHANG Lai-qi, YANG Wang-yue, et al. Criteria of in-situ synthesize of $SiC_p/MoSi_2$ composite [J]. Acta Metallurgica Sinica, 1999, 35: 393- 396.

[2] ZHANG Lai-qi, SUN Zu-qing, YANG Wang-yue, et al. Densification and microstructure of in-situ synthesized $SiC_p/MoSi_2$ composite [J]. Acta Metallurgica Sinica, 1999, 35: 408- 411.

[3] ZHANG Lai-qi, SUN Zu-qing, YANG Wang-yue, et al. Analysis of thermodynamic and kinetic of in-situ synthesized $SiC_p/MoSi_2$ composite [J]. Acta Metallurgica Sinica, 1998, 34: 1205- 1209.

[4] SUN Zu-qing, ZHANG Lai-qi, ZHANG Yue, et al. In-situ synthesis and thermodynamic analysis of $SiC_p/MoSi_2$ composite [A]. Invited presentation, The Third Pacific Rim International Conference on Advanced Materials and Processing [C]. Honolulu, Hawaii, U. S. A., 1998. 305.

[5] SUN Zu-qing, ZHANG Lai-qi Zhang, YANG Wang-yue, et al. Toughening of $SiC_p/MoSi_2$ composite synthesized in situ [J]. Acta Metallurgica Sinica, 2001, 37 (1): 104- 108.

[6] SUN Zu-qing, ZHANG Lai-qi, YANG Wang-yue, et al. Strengthening of $SiC_p/MoSi_2$ composite synthesized in situ at elevated temperature [J]. Acta Metallurgica Sinica, 2001, 37(4): 369- 372.

[7] ZHANG Lai-qi, SUN Zu-qing, ZHANG Yue, et al. Microstructure and mechanical properties of $SiC_p/MoSi_2$ composite synthesized in-situ [J]. Acta Metallurgica Sinica, 2001, 37(3): 325- 331.

[8] Vasudevan A K, Petrovic J J. A comparative overview of molybdenum disilicide composite [J]. Mater Sci Eng, 1992, A155: 1- 17.

[9] LI Jie, YANG G Y, ZHU Jing, et al. Microstructure characterization of sintered $MoSi_0/SiC_p$ composites [J]. J Am Ceram Soc, 2000, 83(4): 992- 994.

[10] Suzuki M, Nutt S R, Aikin R M. Creep behavior of SiC-reinforced XD^{TM} $MoSi_2$ composite [J]. Mat Res Soc Symp Proc, 1992, 273: 267.

[11] Sadanada K, Jone H, Feng J. Creep of monolithic and SiC whisker-reinforced $MoSi_2$[J]. Ceram Eng Sci Proc, 1991, 12(9/10): 1671.

[12] Jeng Y L, Lavernia E J, Wolfenstine J. Creep behavior of plasma-sprayed SiC-reinforced $MoSi_2$ [J]. Scripta Metall, 1993, 29: 107- 111.

(Edited by YANG Bing)